Effects of Inclusion of Granulated Rubber Tyres on the Mechanical Behaviour of a Compressive Sand

W. Li[1], C.Y. Kwok[1*], K. Senetakis[2]

[1] Department of Civil Engineering, The University of Hong Kong, Hong Kong

[2] Department of Architecture and Civil Engineering, City University of Hong Kong, Hong Kong

[*] Corresponding author

Author lists:

W. Li[1], Department of Civil Engineering, The University of Hong Kong, Hong Kong. liwei890508@126.com.

C. Y. Kwok[1*], Department of Civil Engineering, The University of Hong Kong, Hong Kong.

*Corresponding author: fiona.kwok@hku.hk, Tel: +852 2859 2265

K. Senetakis[2], Department of Architecture and Civil Engineering, City University of Hong Kong, Hong Kong. ksenetak@cityu.edu.hk.

ABSTRACT

Drained triaxial shearing tests were performed in this research on a well-graded compressive sand, completely decomposed granite (CDG), and its mixtures with granulated rubber tyres, to investigate the effects of rubber size and content on their mechanical behaviour. Three sizes of rubber particles, GR1, GR2 and GR3, were used with size ratios to CDG ($D_{50,rubber}$: $D_{50,CDG}$) of 0.9, 3.5, 7.2, respectively and the rubber content ranged from 0 to 30%. The results show that, for CDG-GR1 mixtures, the strength decreases with increasing rubber content; while for CDG-GR2 and CDG-GR3 mixtures, the strength decreases only at 10% rubber content and then increases markedly with increasing rubber content. The increase of strength is mainly because the inclusion of large rubber particles widens the particle size distributions of the mixtures, resulting in denser packings. The denser packings also lead to a decrease in compressibility. At larger size ratio and higher rubber content, the CDG-rubber mixtures show higher shear strength and lower compressibility than pure CDG, which indicates the CDG-rubber mixtures are very suitable to be used as filling materials.

Keywords: granulated rubber tyres; compressive sand; mechanical behaviour; filling materials.

1 INTRODUCTION

Every year, over 1 billion tyres are discarded worldwide (WBCSD 2010), consuming lots of space and leading to environmental problems. So, the reuse of scrap rubber tyres has gained popularity. Due to its inherent attractive engineering properties, such as high durability, high permeability, and low bulk density, scrap tyres could be mixed with soil as backfilling materials in retaining walls to reduce the lateral earth pressures (Humphrey and Sandford 1993; Kaneda et al. 2007); lightweight construction materials in embankments to reduce settlements (Lee et al. 1999; Yoon et al. 2006; Edinçliler et al. 2010); and also isolation systems to modify the seismic response of foundations (Tsang et al. 2012; Manohar et al. 2014; Anbazhagan et al. 2015).

The mechanical behaviour of sand-rubber mixtures has been explored extensively in the literature. It has been consistently reported that the rubber shreds or chips, tend to enhance the shear strength of the mixture (Foose et al. 1996; Zornberg et al. 2004; Ghazavi and Sakhi 2005; Bali Reddy et al. 2015), mainly due to the reinforcement effect, while for the granulated rubber particles, there are some contradicting results. Studies from triaxial tests reported that the inclusion of the granulated rubber particles tends to reduce the shear strength of the mixture because of the soft nature of the rubber particles (Youwai and Bergado 2003; Lee et al. 2007; Neaz Sheikh et al. 2013; Noorzad and Raveshi, 2017; Zhang et al. 2018). However, some other studies from direct shear tests showed that the shear strength increases when mixing the sand with granulated rubber particles (Ghazavi 2004; Attom 2006; Anbazhagan and Manohar 2015; Anbazhagan et al. 2014, 2017). Based on the published results from laboratory tests, there is no agreement on how the granulated rubber affects the mechanical behaviour of sand-rubber mixtures, which is worth investigating further.

In most of the previous studies, the rubber particles were mixed with quartzitic sands, which are generally dilative under shearing. However, the availability and cost-efficiency

decide mostly the type of host sand to be used. In tropical/sub-tropical regions, like Hong Kong, completely decomposed granite (CDG) is one of the most common geo-materials for filling/backfilling (Lumb 1962; Yan and Li 2012). CDG is easy to break, and it is generally compressive under shearing. Fu et al. (2014) and Li et al. (2019) both reported that the inclusion of granulated rubber particles had an insignificant effect on the strength of CDG, which differs a lot with the effects on the dilative sands. However, both studies did not consider the effect of rubber size, which has been proved in the literature to be a key factor influencing the behaviour of sand-rubber mixtures in a wide range of strains (Kim and Santamarina 2008; Senetakis et al. 2012), and this was another motivation of this study.

The understanding of the effects of rubber size and content on the mechanical behaviour of a well-graded compressive sand (CDG), could provide more comprehensive guidance for engineering projects where the composite will be used as filling materials. A series of drained triaxial shearing tests were conducted on the CDG-granulated rubber mixtures, considering various rubber sizes and contents. The shear strength and compressibility of the CDG-rubber mixtures were discussed within the critical state framework.

2 MATERIALS AND TESTING PROCEDURES

The host sand used in this study was a well-graded CDG (coefficient of uniformity C_u=6.3, coefficient of curvature C_c=1.2, and D_{50}=0.51mm) from Hong Kong. Three sizes of granulated rubber particles were used: GR1 (0.3-0.6 mm), GR2 (1.18-2.36 mm) and GR3 (2.36-5 mm) to mix with CDG. Figure 1(a) shows the particle size distribution curves of all the materials tested. The size ratios, $D_{50,rubber}$: $D_{50,CDG}$, are about 0.9, 3.5, 7.2 for GR1, GR2 and GR3, respectively. Figure 1(b) shows the images of the CDG and rubber particles, which are both angular to sub-angular in shape. The specific gravities (G_s) were measured following ASTM (2002) standard D854, showing that for CDG is 2.65, and for rubber particles are 1.15.

Triaxial tests were performed on both CDG and its mixtures with granulated rubber tyres (GR1/GR2/GR3) with rubber content of 10%, 20% or 30% by weight of dry mixture. Note that 30% rubber by weight corresponds to 50% by volume, approximately, and it has been considered as a limit, above which the composite will show rubber dominant behaviour (Anastasiadis et al. 2012; Senetakis et al. 2012; Lopera Perez et al. 2016, 2017). For the CDG-rubber mixtures, the CDG and rubber particles were mixed with a small amount of water to prevent segregation. All the specimens (38 mm diameter × 76 mm height) were prepared on the triaxial pedestal directly, using under-compaction method (Ladd 1978). After carbon dioxide and de-air water flushing, back pressure was applied (typically of about 300 kPa) to saturate the specimen, until B values over 0.95 were achieved. After saturation, all the specimens were isotropically consolidated at 50-400 kPa confining pressures and then sheared under a drained condition with a shearing rate of 0.02 mm/min.

3 RESULTS AND DISCUSSION

3.1 Stress-strain behaviour

The stress-strain data of the CDG and its rubber mixtures are shown in Fig. 2. For clearness, only those specimens sheared at mean effective stress p'_c=400 kPa are presented. From small to moderate strain levels, it can be seen that the inclusion of rubber particles all tends to reduce the stiffness of the mixtures (see Figs. 2a, 2c and 2e), which is consistent with the results from many other studies (Youwai and Bergado 2003; Lee et al. 2007; Neaz Sheikh et al. 2013; Anbazhagan and Manohar 2016), mainly due to the strong force chain going through softer rubber particles. With the increasing rubber content, the stronger force chain goes through more rubber particles, so that the stiffness reduces more pronouncedly. While this trend contradicts some findings from direct shear tests (Attom 2006; Edincliler et al. 2010; Anbazhagan et al. 2017), in which it was stated that the inclusion of rubber particles

tends to enhance the stiffness of the mixtures. However, in those studies the mechanism was not discussed in detail. It is possible that the rubber particle size and stiffness are different, or the behaviour of the host sand affects significantly the response of the mixtures as reported by Anbazhagan et al. (2017). In Fig. 3(a), it is shown that, with the same rubber content, larger rubber particles lead to less reduction in stiffness. This behaviour is speculated to be because the larger rubber particles have smaller specific areas, resulting in fewer sand-rubber contacts (Lopera Perez et al. 2017), so that the strong force chains go through fewer rubber particles, resulting in less reduction in stiffness.

From moderate to large strain levels, all the specimens show slight post peak strain softening behaviour, with very close stresses at the peak and critical states. The axial strain corresponding to peak stress increases with the increasing rubber content, indicating higher ductility which is important when the sand-rubber mixtures are applied for seismic isolation (Tsang et al. 2012). For CDG-GR1 mixtures, the stresses at both the peak and critical states decrease slightly with the increase of rubber content. While for CDG-GR2/GR3 mixtures, the peak stress shows an increasing trend with the increasing rubber content. Although the findings contradict the results of those testing granulated rubber particles mixed with dilative sands (Youwai and Bergado 2003; Neaz Sheikh et al. 2013; Noorzad and Raveshi 2017), it is under expectation to some extent. For those tested granulated rubber mixing with dilative sands, it was found that the reduction in shear strength can be minimized by using larger granulated rubber particles (Neaz Sheikh et al. 2013). Meanwhile, Li et al. (2019) tested compressive sands mixing with similar sized granulated rubber particles and reported that the strength reduction was insignificant. So, it is reasonable to expect that the larger granulated rubber particles can have some favourable effects when mixing with a compressive sand.

Note that there are also some results from direct shear tests showing similar trends with the current study that the shear strength increases when adding granulated rubber particles

into the sand up to a certain content (Ghazavi 2004; Attom 2006; Anbazhagan and Manohar 2015; Anbazhagan et al. 2014, 2017). This rubber content is treated as the optimum rubber content, beyond which the shear strength will reduce. Anbazhagan and Manohar (2015) and Anbazhagan et al. (2017) reported that the optimum rubber content is about 15% by weight. However, in this study, the shear strength increases with increasing rubber content up to 30% by weight. This might be attributed to the initial loose state of the host sand. Since it was found in Anbazhagan et al. (2017) that the inclusion of rubber particles benefits more when the initial state of the host sand is less dilative, so it is possible for the contractive CDG specimens (much looser) to accommodate more rubber particles to achieve their densest state and highest shear strength. The behaviour will be discussed further in terms of mobilized friction angles in the subsequent section.

For the volumetric strain behaviour, both CDG and its rubber mixtures are nearly pure contractive (see Figs. 2b, 2d and 2f). For CDG, the contraction comes from the breakage of particles; while for CDG-rubber mixture, the contraction is attributed to both the breakage of CDG particles and the high deformability of rubber particles. It is noted that the contraction due to the deformation of rubber particles, which contributes in filling the void spaces of the solid matrix, becomes more pronounced; while the contraction from particle breakage becomes less pronounced because the inclusion of rubber particles tends to suppress particle breakage. Figure 3(b) shows that the contraction becomes less with the increasing rubber size. The explanations will also be provided in the subsequent section.

3.2 Shear strength at the peak

In this section, the shear strength before and after rubber inclusion is discussed in terms of mobilized friction angles at the peak (φ'_p) and critical states (φ'_{cs}). The following shows briefly how to obtain φ'_p and φ'_{cs}, using pure CDG as an example. Figure 4 shows the stress

paths of pure CDG specimens sheared from different confining pressures, in which the peak and critical states are marked. The φ'_p and φ'_{cs} are obtained by:

$$\sin\varphi'_p = 3M_p / (6 + M_p) \quad (1)$$

$$\sin\varphi'_{cs} = 3M_{cs} / (6 + M_{cs}) \quad (2)$$

where M_p and M_{cs} are the gradient of the peak and critical state lines, respectively. Note that the peak line is tentative here, which helps to assess the average peak strength of the material. The effect of initial densities on the peak stress will be discussed subsequently. Table 1 summarizes the values of φ'_p and φ'_{cs} for the CDG and its rubber mixtures.

Figure 5 shows the responses of peak strength to rubber size and content. When the CDG and rubber have a similar particle size ($D_{50,rubber}$: $D_{50,CDG}$ = 0.9), in general, φ'_p decreases slightly with increasing rubber content. Li et al. (2019) adopted the theory by Terzaghi et al (1996), stating that the shear strength (φ'_{mob}) is mobilized from inter-particle friction (φ'_μ), dilation (φ'_d) and particle rearrangement (φ'_b), i.e. $\varphi'_{mob} = \varphi'_\mu + \varphi'_d + \varphi'_b$, to explain the effects of rubber inclusion on the mechanical behaviour of sands. It was reported that rubber particles have smaller φ'_μ than CDG, hence the inclusion of rubber into CDG would lower the φ'_μ. On the other hand, the rubber particles suppress the breakage of CDG particles and thus lead to higher strength mobilized from particle rearrangement (i.e. higher φ'_b). The inclusion of rubber does not cause any dilatancy, therefore φ'_d is insignificant similar to that of pure CDG. The decrease of φ'_μ is more pronounced than the increase of φ'_b resulting in the overall decrease of φ'_p. However, the effect of rubber size was not considered in Li et al. (2019).

At higher size ratios (3.5 and 7.2), φ'_p shows a slight reduction only at 10% rubber content and then increases markedly with increasing rubber content. The mixture with a size ratio of 7.2 and rubber content of 30% shows the highest φ'_p. If we adopt Li et al (2019)'s explanation, the inclusion of larger rubber particles only leads to fewer sand-rubber and

rubber-rubber contacts, resulting in less reduction in inter-particle friction. However, it cannot explain the higher peak strength of CDG-rubber mixtures in comparison to pure CDG.

Generally, it has been considered that both φ'_d and φ'_b are influenced strongly by the packing density (Been and Jefferies 1985), and the packing density is found to increase when the particle size distribution is wider (Sohn and Moreland 1968). For these CDG-rubber mixtures, the particle size distributions become narrower (lower C_u) with increasing GR1 content; while the particle size distributions become wider (higher C_u) with increasing GR2/GR3 content. All the C_u values are presented in Table 1. Figure 6 plots the φ'_p against C_u for pure CDG and CDG-rubber mixtures. It shows that there is an approximately linear relationship between φ'_p and C_u, and the material with higher C_u value shows higher peak strength. These observations are mainly because the particle size distributions become wider after the inclusion of GR2/GR3, leading to denser packings so that the particle rearrangement becomes harder and particle breakage becomes less (higher φ'_b). Also, because of the denser packing, the contraction becomes less with the increasing rubber size (higher φ'_d), as shown already in Figure 3(b). The responses of shear strength at the critical state (φ'_{cs}) to rubber size and content are almost the same with those of φ'_p. However, due to the contribution of particle rearrangement is less at the critical state in comparison to the peak, so the effect of the reduction in inter-particle friction becomes more pronounced.

3.3 Critical state lines in v-lnp' space

Figures 7 shows the compression and shearing paths of CDG and its rubber mixtures, where the critical states are marked. It can be seen that a unique CSL can be defined for each material. The gradient, λ, and the intercept at 1 kPa, Γ, of the CSL are also included in Table 1. In Fig. 7(a), for CDG-GR1 mixtures, the CSL moves downwards when the rubber content increases. The gradient λ, which indicates the compressibility of the material does not change much when the GR1 content is 10%. As the GR1 content goes to 20% or 30%, λ values are

higher, indicating higher compressibility. Figure 7(b) shows that, at 30% rubber content, the CSL also moves downwards with increasing rubber size; while λ of CDG-GR2/GR3 is lower than that of pure CDG, indicating lower compressibility. Figure 8 plots λ against C_u. It shows that the material with higher C_u value shows lower gradient λ. It can again be explained that the higher C_u value results in denser packing, leading to less compression and less particle breakage (i.e. lower compressibility).

3.4 Peak strength with respect to the state parameter

In this section, the peak strength was discussed further with respect to the state parameter, proposed by Been and Jefferies (1985), which considers the effects of initial void ratio and stress level. The state parameter (ψ) is the difference between the current void ratio (e_c) and the void ratio at the critical state (e_{cs}) of a soil at the same mean effective stress level, i.e. $\psi = e_c - e_{cs}$. Figure 9 shows the peak strength against state parameters. It can be seen that the peak strength decreases with the increase of state parameter for all the materials tested. Within some scatteredness, a unique relationship can be identified for all the materials, which indicates that the major effect of rubber inclusion to those mixtures is the change of particle packing due to the alteration of particle size distribution. For CDG-GR2/GR3 mixtures, especially at 30% rubber content, the state parameters decrease obviously, indicating denser packing, which results in higher peak strength.

3.5 Feasibility of using CDG-rubber mixtures as filling materials

In the above sections, the shear strength and compressibility of CDG-rubber mixtures were thoroughly discussed. At larger rubber-sand size ratio and higher rubber content, it was found that the compressibility is lower, and the shear strength is higher than those of pure CDG. This indicates that CDG-rubber mixtures are very good geo-materials considering the

shear strength and the compressibility, especially in Hong Kong where CDG is widely distributed and can be easily obtained. More importantly, if the waste tyres mixed with CDG in the granulated/shredded form can be used as filling geosynthetic, it can save lots of valuable space for the tyre disposal and create new land at the same time.

4 CONCLUSIONS

A series of triaxial shearing tests were conducted on a well-graded CDG and different CDG-rubber mixtures, to examine the effects of rubber particle size and content on the mechanical behaviour of CDG, which confirms the feasibility of using CDG-rubber mixtures as filling materials, especially when using larger rubber particles. The main points are summarised below:

(1) Regarding the stiffness, all the CDG-rubber mixtures show softer responses than the pure CDG, which is more obvious with the increasing rubber content. At the same rubber content, the mixture with larger rubber particles shows higher stiffness, due to fewer soft rubber particles involved in the formation of strong force chain.

(2) Regarding the peak strength (φ'_p), the φ'_p decreases slightly with increasing of rubber content when the CDG and rubber have similar particle size; while it shows an increasing trend with increasing rubber content when mixing with larger rubber particles. The particle size distribution of the CDG-rubber mixtures is found to affect the φ'_p markedly and it is explained that the inclusion of larger rubber particles leads to wider particle size distributions, so that the packing becomes denser and the particle rearrangement becomes harder, resulting in higher peak strength.

(3) Regarding the compressibility, it increases with increasing rubber content when the CDG and rubber have similar particle size; while after adding larger rubber particles, the compressibility reduces with increasing rubber content. It can also be explained that the

inclusion of larger rubber particles leads to wider particle size distributions, resulting in denser packing so that less void space for compression and less particle breakage (i.e. lower compressibility).

ACKNOWLEDGEMENT

This study was supported by the Environment and Conservation Fund (ECF) under the project 'Recycling tyre waste as a useful geo-material to enhance sustainability' (Project number 55/2016). The authors acknowledge a grant from the Research Grants Council of the Hong Kong Special Administrative Region (Project number 11206617).

NOTATION

C_c coefficient of curvature

CDG completely decomposed granite

CSL critical state line

C_u coefficient of uniformity

D_{50} mean particle size

e void ratio

e_c current void ratio

e_{cs} void ratio at critical state

G_s specific gravity

M_{cs} slope of the CSL in q:p' plane

M_p slope of the peak line in q:p' plane

p' mean effective stress

p'_c mean effective stress the specimen sheared from

q deviatoric stress

v_0 initial specific volume

λ gradient of the CSL

φ'_b friction angle mobilized from particle rearrangement

φ'_{cs} friction angle at the critical state

φ'_d friction angle mobilized from dilation

φ'_p peak friction angle

φ'_μ inter-particle friction angle

ψ state parameter

Γ intercept at 1 kPa of the CSL

REFERENCES

Anastasiadis, A., Senetakis, K., and Pitilakis, K. 2012. Small-strain shear modulus and damping ratio of sand-rubber and gravel-rubber mixtures. Geotechnical and Geological Engineering, **30** (2), 363–382. doi:10.1007/s10706-011-9473-2.

Anbazhagan, P., Manohar, D.R., and Divyesh, R. 2017. Influence of size of granulated rubber and tyre chips on the shear strength characteristics of sand-rubber mix. Geomechanics and Geoengineering: An International Journal, **12**(4), 266–278. doi:10.1080/17486025.2016.1222454.

Anbazhagan, P., and Manohar, D.R. 2015. Energy absorption capacity and shear strength characteristics of waste tire crumbs and sand mixtures. International Journal of Earthquake Geotechnical Engineering, **6**(1), 28–49. doi:10.4018/IJGEE.2015010103.

Anbazhagan, P., Manohar, D.R., and Neaz Sheikh, M. 2014. Response surface analysis for engineering behavior of sand-tire crumb mixtures. *In* Proceedings of 2nd International Conference on Information Technology in Geo-Engineering, Durham, UK, pp. 260–265.

Anbazhagan, P., and Manohar, D.R. 2016. Small- to large-strain shear modulus and damping ratio of sand-tyre crumb mixtures. *In* Proceedings of Geo-Chicago 2016, Chicago, pp. 305–315.

Anbazhagan, P., Manohar, D.R., and Divyesh, R. 2015. Low cost damping scheme for low to medium rise buildings using rubber soil mixtures. *In* Proceedings of Second Japan-India Workshop in Geotechnical Engineering - Geotechnics for Resilient Infrastructure, Fukuoka University, Japan, pp. 23–27.

ASTM. 2002. Standard test methods for specific gravity of soil solids by water pycnometer. ASTM standard D854. Annual book of ASTM standards. American Society for Testing and Materials, West Conshohocken, Pa.

Attom, M.F. 2006. The use of shredded waste tires to improve the geotechnical engineering properties of sands. Environmental Geology, **49**(4), 497–503. doi:10.1007/s00254-005-0003-5.

Bali Reddy, S., Pradeep Kumar, D., and Murali Krishna, A. 2015. Evaluation of the optimum mixing ratio of a sand-tire chips mixture for geoengineering applications. Journal of Materials in Civil Engineering, **28**(2), 06015007. doi:10.1061/(ASCE)MT.1943-5533.0001335.

Been, K., and Jefferies, M.G. 1985. A state parameter for sands. Géotechnique, **35**(2), 99–112. doi:10.1680/geot.1985.35.2.99.

Edinçliler, A., Baykal, G., and Saygılı, A. 2010. Influence of different processing techniques on the mechanical properties of used tires in embankment construction. Waste Management, **30**(6), 1073–1080. doi:10.1016/j.wasman.2009.09.031.

Foose, G.J., Benson, C.H., and Bosscher, P.J. 1996. Sand reinforced with shredded waste tires. Journal of Geotechnical Engineering, **122**(9), 760–767. doi:10.1061/(ASCE)0733-9410(1996)122:9(760).

Fu, R., Coop, M.R., and Li, X.Q. 2014. The mechanics of a compressive sand mixed with tyre rubber. Géotechnique Letters, **4**(3), 238–243. doi:10.1680/geolett.14.00027.

Ghazavi, M. 2004. Shear strength characteristics of sand-mixed with granular rubber. Geotechnical & Geological Engineering, **22**(3), 401–416. doi:10.1023/B:GEGE.0000025035.74092.6c.

Ghazavi, M., and Sakhi, M.A. 2005. Influence of optimized tire shreds on shear strength parameters of sand. International Journal of Geomechanics, **5**(1), 58–65. doi:10.1061/(ASCE)1532-3641(2005)5:1(58).

Humphrey, D., and Sandford, T. 1993. Tire chips as lightweight subgrade fill and retaining wall backfill. *In* Proceedings of the Symposium on Recovery and Effective Reuse of

Discarded Materials and By-Products for Construction of Highway Facilities, Denver, USA, pp.19–22.

Kaneda, K., Hazarika, H., and Yamazaki, H. 2007. The numerical simulation of earth pressure reduction using tire chips in backfill. *In* Proceedings of the International Workshop on Scrap Tire Derived Geomaterials-Opportunities and Challenges, Yokosuka, Japan, pp. 245–251.

Kim, H.K., and Santamarina, J.C. 2008. Sand-rubber mixtures (large rubber chips). Canadian Geotechnical Journal, **45**(10), 1457–1466. doi:10.1139/T08-070.

Ladd, R.S. 1978. Preparing test specimens using undercompaction. Geotechnical Testing Journal, **1**(1), 16–23. doi:10.1520/GTJ10364J.

Lee, J.H., Salgado, R., Bernal, A., and Lovell, C.W. 1999. Shredded tires and rubber-sand as lightweight backfill. Journal of Geotechnical and Geoenvironmental Engineering, **125**(2), 132–141. doi:10.1061/(ASCE)1090-0241(1999)125:2(132).

Lee, J.S., Dodds, J., and Santamarina, J.C. 2007. Behavior of rigid-soft particle mixtures. Journal of Materials in Civil Engineering, **19**(2), 179–184. doi:10.1061/(ASCE)0899-1561(2007)19:2(179).

Li, W., Kwok, C.Y., Sandeep, C.S., and Senetakis, K. 2019. Sand type effect on the behaviour of sand-granulated rubber mixtures: Integrated study from micro-to macro-scales. Powder Technology, **342**, 907–916. doi:10.1016/j.powtec.2018.10.025.

Lopera Perez, J.C., Kwok, C.Y., and Senetakis, K. 2016. Effect of rubber size on the behavior of sand-rubber mixtures: a numerical investigation. Computers and Geotechnics, **80**, 199–214. doi:10.1016/j.compgeo.2016.07.005.

Lopera Perez, J.C., Kwok, C.Y., and Senetakis, K. 2017. Micromechanical analyses of the effect of rubber size and content on sand-rubber mixtures at the critical state. Geotextiles and Geomembranes, **45**(2), 81–97. doi:10.1016/j.geotexmem.2016.11.005.

Lumb, P. 1962. The properties of decomposed granite. Géotechnique, **12**(3), 226–243. doi:10.1680/geot.1962.12.3.226.

Manohar, D.R., Anbazhagan, P., Neaz Sheikh, M., and Tsang, H.H. 2014. Effects of geosynthetic reinforcement on the mechanical behaviour of composite materials for vibration isolation. *In* Proceedings of the 23rd Australasian Conference on the Mechanics of Structures and Materials, Byron Bay, Australia, pp. 217–222.

Neaz Sheikh, M., Mashiri, M.S., Vinod, J.S., and Tsang, H.H. 2013. Shear and compressibility behavior of sand–tire crumb mixtures. Journal of Materials in Civil Engineering, **25**(10), 1366–1374. doi:10.1061/(ASCE)MT.1943-5533.0000696.

Noorzad, R., and Raveshi, M. 2017. Mechanical behavior of waste tire crumbs-sand mixtures determined by triaxial tests. Geotechnical and Geological Engineering, **35**(4), 1793–1802. doi:10.1007/s10706-017-0209-9.

Senetakis, K., Anastasiadis, A., and Pitilakis K. 2012. Dynamic properties of sand/rubber (SRM) and gravel/rubber (GRM) mixtures in a wide range of shearing strain amplitudes. Soil Dynamics and Earthquake Engineering, **33**(1), 38–53. doi:10.1016/j.soildyn.2011.10.003.

Sohn, H.Y., and Moreland, C. 1968. The effect of particle size distribution on packing density. The Canadian Journal of Chemical Engineering, **46**(3), 162–167. doi:10.1002/cjce.5450460305.

Terzaghi, K., Peck, R.B., and Mesri, G. 1996. Soil mechanics in engineering practice. John Wiley & Sons.

Tsang, H.H., Lo, S.H., Xu, X., and Neaz Sheikh, M. 2012. Seismic isolation for low-to-medium-rise buildings using granulated rubber-soil mixtures: numerical study. Earthquake Engineering & Structural Dynamics, **41**(14), 2009–2024. doi:10.1002/eqe.2171.

WBCSD (World Business Council for Sustainable Development). 2010. End of life tires: a framework for effective management systems [online]. Available from https://docs.wbcsd.org/2010/10/AFrameworkForEffectiveManagementSystems.pdf [cited 25 June 2019].

Yan, W.M., and Li, X.S. 2012. Mechanical response of a medium-fine-grained decomposed granite in Hong Kong. Engineering geology, **129**, 1–8. doi:10.1016/j.enggeo.2011.12.013.

Yoon, S., Prezzi, M., Siddiki, N.Z., and Kim, B. 2006. Construction of a test embankment using a sand–tire shred mixture as fill material. Waste Management, **26**(9), 1033–1044. doi:10.1016/j.wasman.2005.10.009.

Youwai, S., and Bergado, D.T. 2003. Strength and deformation characteristics of shredded rubber tire-sand mixtures. Canadian Geotechnical Journal, **40**(2), 254–264. doi:10.1139/t02-104.

Zhang, T., Cai, G., and Duan, W. 2018. Strength and microstructure characteristics of the recycled rubber tire-sand mixtures as lightweight backfill. Environmental Science and Pollution Research, **25**(4), 3872–3883. doi:10.1007/s11356-017-0742-3.

Zornberg, J.G., Cabral, A.R., and Viratjandr, C. 2004. Behaviour of tire shred-sand mixtures. Canadian Geotechnical Journal, **41**(2), 227–241. doi:10.1139/t03-086.

LIST OF TABLES

LIST OF FIGURES

Table 1. Peak and critical state parameters

Material	φ'_p	φ'_{cs}	λ	Γ	C_u
CDG	37.3°	36.2°	0.127	2.505	6.2
10%GR1	36.4°	33.9°	0.125	2.431	4.7
20%GR1	36.9°	33.4°	0.152	2.463	3.8
30%GR1	35.9°	32.1°	0.162	2.471	3.3
10%GR2	36.9°	33.4°	0.102	2.138	6.8
20%GR2	38.0°	36.4°	0.113	2.089	7.6
30%GR2	38.7°	36.9°	0.103	1.990	8.4
10%GR3	36.9°	34.6°	0.101	2.139	6.8
20%GR3	37.8°	35.7°	0.101	2.009	7.6
30%GR3	39.2°	37.3°	0.095	1.883	11.2

Note: φ'_p peak friction angle, φ'_{cs} friction angle at the critical state, λ and Γ the gradient and the intercept at 1 kPa of the critical state line, respectively, C_u coefficient of uniformity.

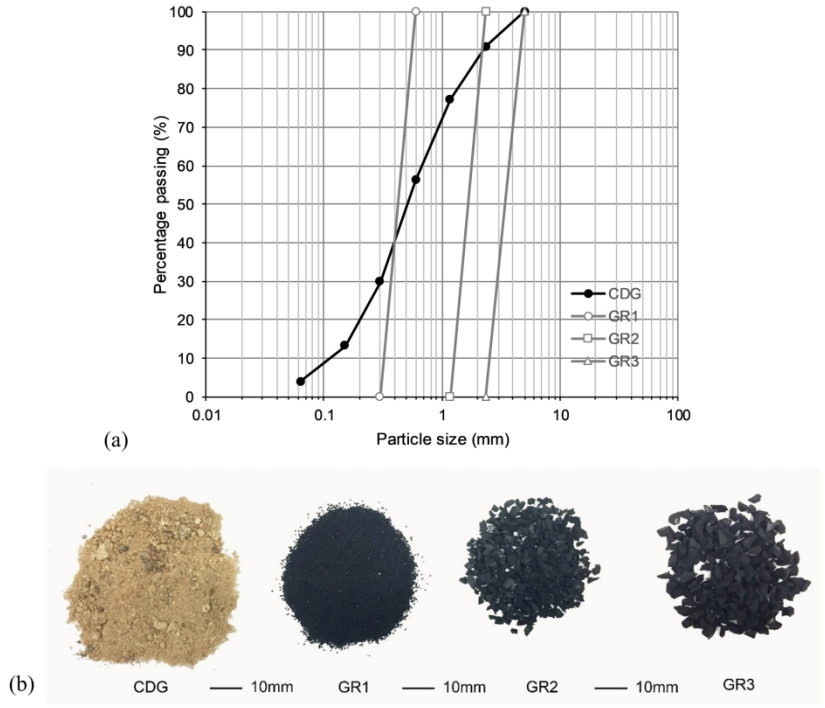

Fig. 1. Materials used: (a) particle size distribution and (b) images of particles.

254x190mm (300 x 300 DPI)

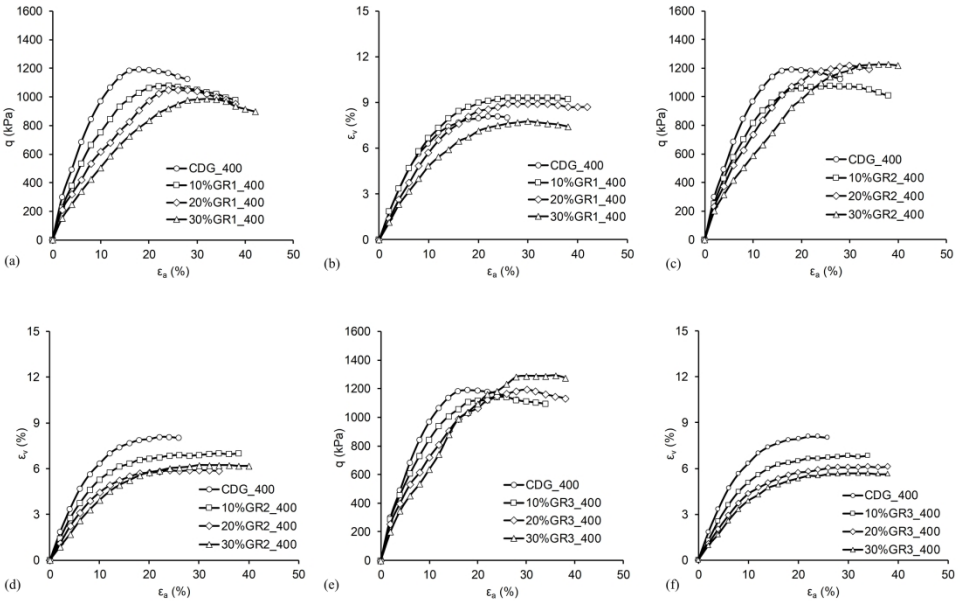

Fig. 2. Stress-strain: (a) GR1, (c) GR2 and (e) GR3, and volumetric strain: (b) GR1, (d) GR2 and (f) GR3, behaviour of CDG-rubber mixtures sheared at p'c = 400 kPa (with pure CDG for comparison).

254x190mm (300 x 300 DPI)

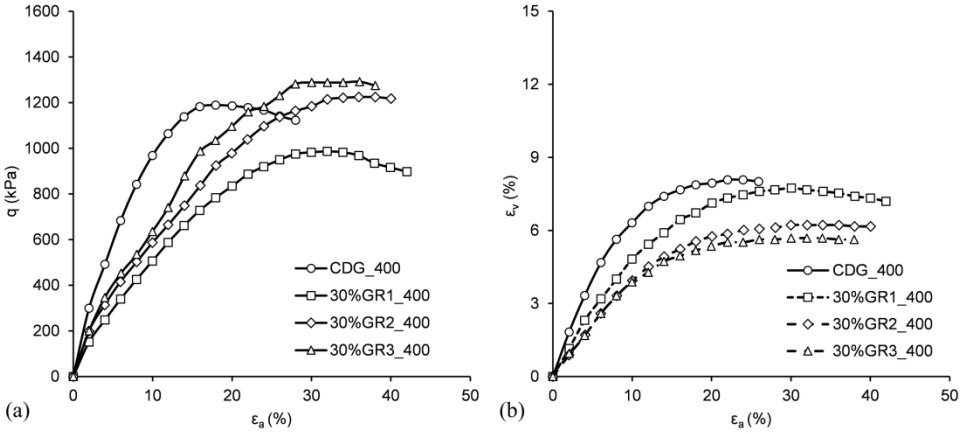

Fig. 3. (a) Stress-strain and (b) volumetric strain behaviour of CDG-rubber mixtures at 30% rubber content and sheared at p'c = 400 kPa (with pure CDG for comparison).

254x190mm (300 x 300 DPI)

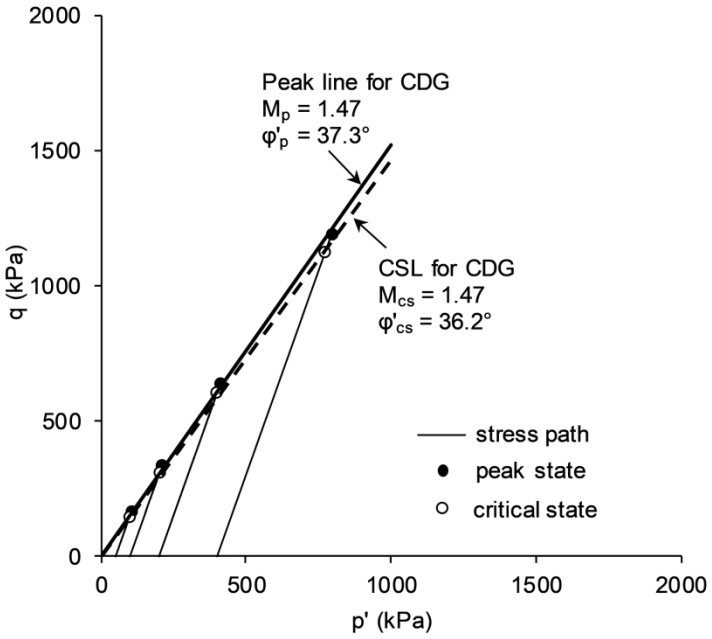

Fig. 4. Stress paths of pure CDG specimens under shearing.

254x190mm (300 x 300 DPI)

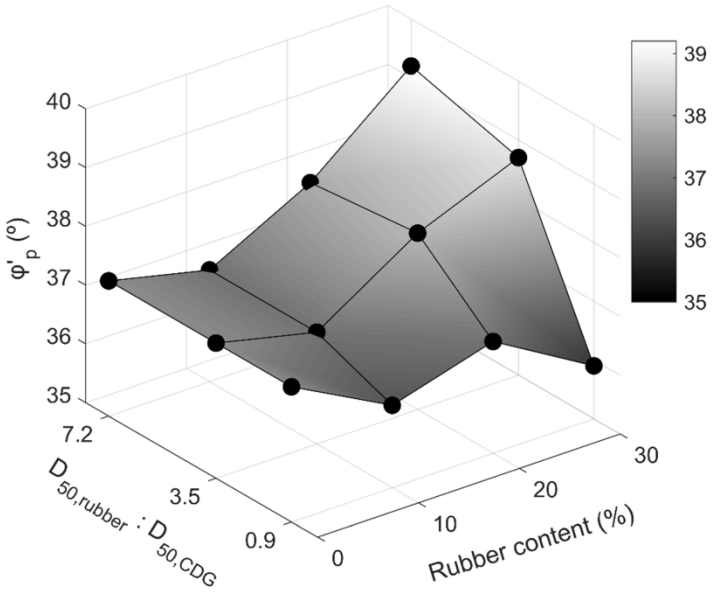

Fig. 5. Responses of peak strength to rubber size and content.

254x190mm (300 x 300 DPI)

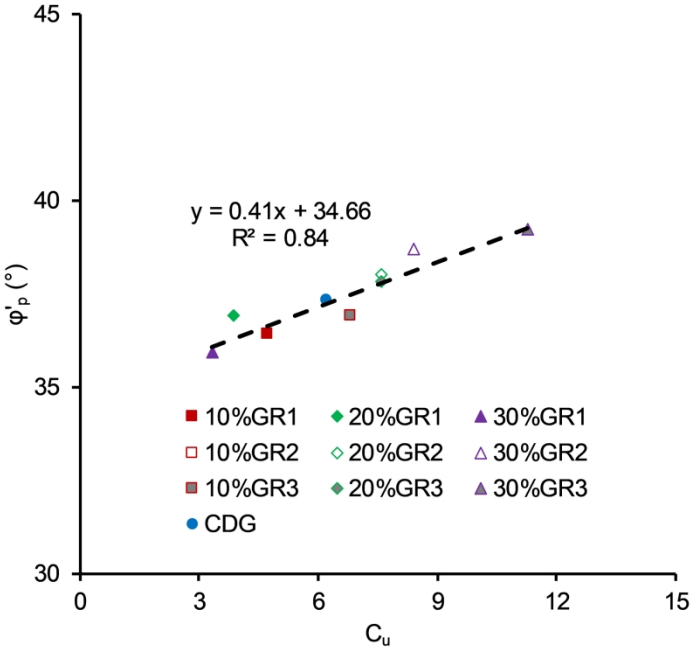

Fig. 6. Relationship between φ'p and coefficient of uniformity (Cu).

254x190mm (300 x 300 DPI)

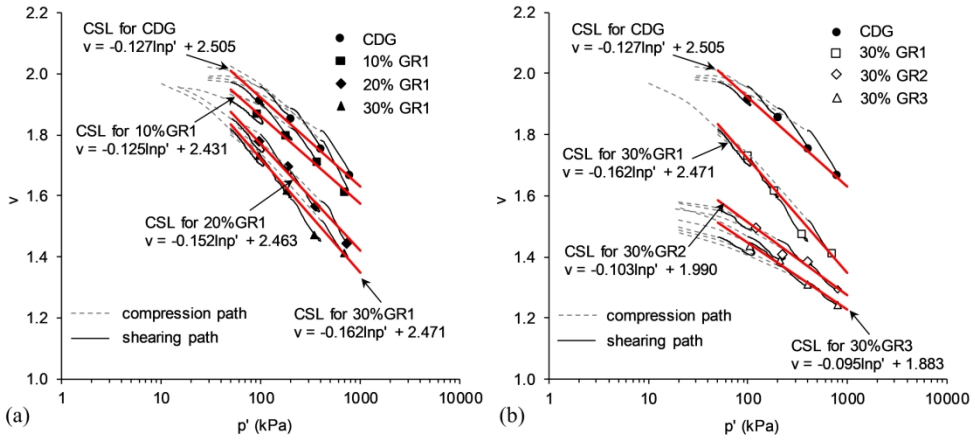

Fig. 7. Critical state lines for: (a) pure CDG and CDG-GR1 mixtures and (b) pure CDG and CDG-rubber mixtures (GR1/GR2/GR3) with 30% rubber content.

254x190mm (300 x 300 DPI)

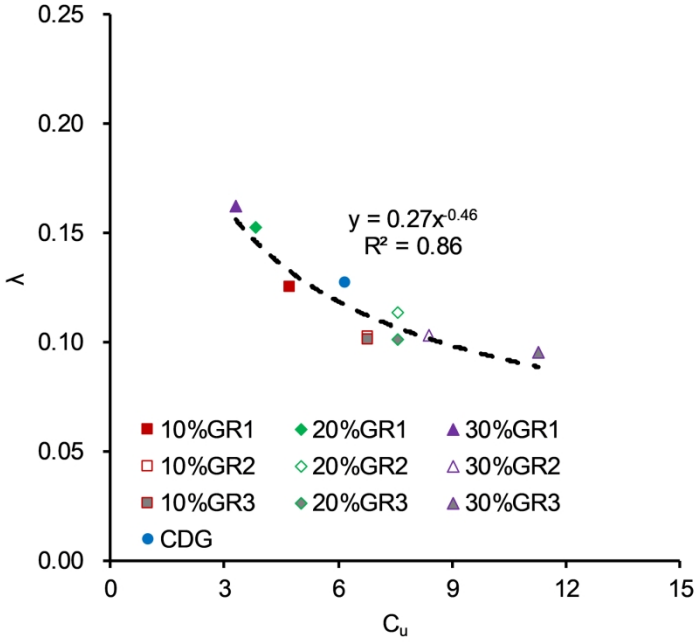

Fig. 8. Relationship between λ and Cu.

254x190mm (300 x 300 DPI)

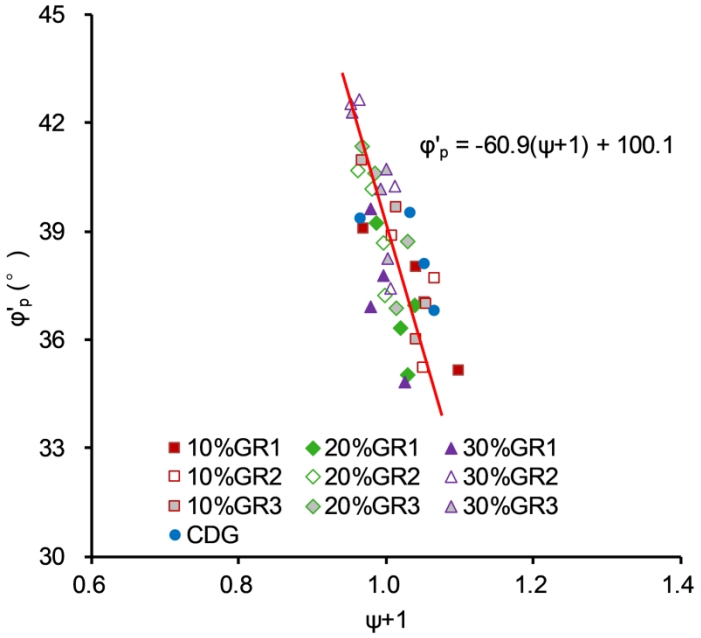

Fig. 9. The relationship between peak strength φ'p and state parameter+1 (ψ+1) for CDG and its rubber mixtures.

254x190mm (300 x 300 DPI)